

Article

Berry Phase of Two Impurity Qubits as a Signature of Dicke Quantum Phase Transition

Wangjun Lu ^{1,2} , Cuilu Zhai ¹, Yan Liu ³, Yaju Song ³, Jibing Yuan ³ and Shiqing Tang ^{3,*}¹ Department of Maths and Physics, Hunan Institute of Engineering, Xiangtan 411104, China² Zhejiang Institute of Modern Physics, Department of Physics, Zhejiang University, Hangzhou 310027, China³ College of Physics and Electronic Engineering, Hengyang Normal University, Hengyang 421002, China

* Correspondence: sqtang@hynu.edu.cn

Abstract: In this paper, we investigate the effect of the Dicke quantum phase transition on the Berry phase of the two impurity qubits. The two impurity qubits only have dispersive interactions with the optical field of the Dicke quantum system. Therefore, the two impurity qubits do not affect the ground state energy of the Dicke Hamiltonian. We find that the Berry phase of the two impurity qubits has a sudden change at the Dicke quantum phase transition point. Therefore, the Berry phase of the two impurity qubits can be used as a phase transition signal for the Dicke quantum phase transition. In addition, the two impurity qubits change differently near the phase transition point at different times. We explain the reason for the different variations by studying the variation of the Berry phase of the two impurity qubits with the phase transition parameters and time. Finally, we investigated the variation of the Berry phases of the two impurity qubits with their initial conditions, and we found that their Berry phases also have abrupt changes with the initial conditions. Since the Dicke quantum phase transition is already experimentally executable, the research in this paper helps to provide a means for manipulating the Berry phase of the two impurity qubits.

Keywords: Berry phase; Dicke quantum phase transition; two impurity qubits; dispersive interaction; X-type state



Citation: Lu, W.; Zhai, C.; Liu, Y.; Song, Y.; Yuan, J.; Tang S. Berry Phase of Two Impurity Qubits as a Signature of Dicke Quantum Phase Transition. *Photonics* **2022**, *9*, 844. <https://doi.org/10.3390/photonics9110844>

Received: 16 October 2022

Accepted: 7 November 2022

Published: 9 November 2022

Publisher's Note: MDPI stays neutral with regard to jurisdictional claims in published maps and institutional affiliations.



Copyright: © 2022 by the authors. Licensee MDPI, Basel, Switzerland. This article is an open access article distributed under the terms and conditions of the Creative Commons Attribution (CC BY) license (<https://creativecommons.org/licenses/by/4.0/>).

1. Introduction

In quantum mechanics, the wave function of a system is determined by the probability amplitude and phase. In 1984, Berry discovered that a quantum system with a time-dependent Hamiltonian has a dynamical phase and an additional phase after adiabatic, unitary, and cyclic evolution [1]. This extra phase is only related to the closed path of the system on the parameter space and is called the Berry phase. Simon then gives a geometric interpretation of the Berry phase [2]. Simon points out that the Berry phase can be regarded as the holonomy of a line bundle L over the space of parameters M of the system if L is endowed with a natural connection [2]. Thus, the Berry phase is also known as the geometric phase. Aharonov and Anandan then showed that for non-adiabatic cyclic evolution, there is also a canonically invariant phase related only to the evolution path [3]. This phase is called the A-A phase. In fact, Pancharatnam discovered this phenomenon in classical optics [4], so the Berry phase is sometimes called the Pancharatnam–Berry phase [5]. Inspired by Pancharatnam's work, Samuel and Bhandari found that the geometric phase can also be defined for acyclic evolution [6]. These phases are experimentally confirmed in systems such as optical and quantum qubits [7–11]. For systems where the initial state is the density matrix, Sjöqvist et al. introduced the geometric phase of the density matrix under the unitary evolution through a hypothetical Mach–Zehnder interferometer experiment [12]. This phase was subsequently confirmed experimentally [13]. Tong et al. further generalized the geometric phase to systems under non-unitary evolution [14]. Since the geometric phase is only path-dependent in parameter space, it can render robust

protocols for quantum computation [15–18], in which quantum computing has a strong advantage over classical computing [19–22].

Furthermore, many experimental and theoretical studies have used Berry phases to detect quantum phase transitions [23–43]. The idea of using the properties of the Berry phase to explore the quantum phase transition was first proposed and applied in the XY spin-1/2 chain model [27,31,33,34]. Carollo and Pachos proposed a method that is theoretically and experimentally capable of detecting critical regions by the geometric phase without requiring the system to undergo a phase transition [27]. They then presented a general form of the relationship between the geometric phase generated by a cyclically evolving interacting spin system and its critical behavior [31]. Zhu established the connection between the ground state geometric phase and the quantum phase transition in general many-body systems [33]. In the Dicke model, Plastina et al. showed that, in the thermodynamic limit, a nonzero Berry phase can be obtained only along a path around a critical point in parameter space [32]. Chen et al. showed that the quantum phase transition characterized by the nonanalytic nature of the geometric phase is a first-order phase transition [36]. In addition, other models that use Berry phases to explore quantum phase transitions include the Lipkin–Meshkov–Glick model [37,38,40], the extended Dicke model [39], and the interacting Fermi model [41,42].

There is a ground state quantum phase transition in the standard Dicke model [44–52]. In addition, the dynamical behavior of impurity atoms in multiple identical atoms has been extensively studied [51,53–65]. Inspired by the abrupt changes in the dynamical behavior of some systems at the quantum phase transition point [66–76], in this paper, we focus on the effect of the Dicke quantum phase transition on the Berry phase of the two impurity qubits (TIQs). We find that the Berry phase of the TIQs has a sudden change at the phase transition point, so the Berry phase of the TIQs can be used as a signal to detect the Dicke quantum phase transition.

This paper is organized as follows. In Section 2, we study the dynamics of the TIQs in a cavity-Bose–Einstein condensate (cavity-BEC) system. Then, we obtain the quantum state and Berry phase of the TIQs at time t . In Section 3, we study the effect of the Dicke quantum phase transition on the TIQs in the cavity-BEC system and find a sudden change in the Berry phase of the TIQs at the phase transition point. We also consider the effect of the initial state of the two qubits on their Berry phase. Finally, we discuss that our scheme is experimentally executable. In Section 4, we conclude the whole paper and point out our future works.

2. Dicke Model with Two Impurity Qubits and Berry Phase of Two Impurity Qubits

In this section, we discuss the effect of the Dicke quantum phase transition on the Berry phase of two two-level atoms. As shown in Figure 1, we consider a cavity-Bose–Einstein condensate system (cavity-BEC) containing two impurity qubits (TIQs), where the BEC consists of N identical two-level atoms. In this case, the TIQs only have dipole interactions with the optical field and do not interact with the atoms. The interaction of two two-level atoms with a single-mode optical field is described by a Tavis–Cummings (TC) model Hamiltonian as follows ($\hbar = 1$):

$$\hat{H}_{TC} = \omega_a \hat{a}^\dagger \hat{a} + \sum_{i=A,B} \frac{\omega_i}{2} \hat{\sigma}_z^i + \Omega \sum_{i=A,B} (\hat{a}^\dagger \hat{\sigma}_-^i + \hat{\sigma}_+^i \hat{a}), \tag{1}$$

where \hat{a} (\hat{a}^\dagger) is the annihilation (creation) operator of the single-mode cavity field with resonance frequency ω_a and $\omega_{A(B)}$ is the transition frequency between the two levels of the i th atom. $\hat{\sigma}_{x,y,z}^i$ are the usual Pauli operators of the i th atom, and $\hat{\sigma}_\pm^i = \frac{1}{2}(\hat{\sigma}_x^i \pm i\hat{\sigma}_y^i)$. Ω is the dipole interaction strength between the cavity field and the single atom. We define a frequency detuning $\delta_{A(B)} = \omega_{A(B)} - \omega_a$. When the frequency detuning $\delta_{A(B)}$ between the two-level atom and cavity field is sufficiently large, i.e., $|\delta_{A(B)}|/\Omega \gg \sqrt{n+1}$

for any “relevant” photon number n [77]. Under this condition, we can obtain the effective dispersive Hamiltonian of the two-atom TC model as follows [77–81]:

$$\hat{H}_{TC}^{eff} = \omega_a \hat{a}^\dagger \hat{a} + \sum_{i=A,B} \frac{\omega_i + \chi_i}{2} \hat{\sigma}_z^i + \sum_{i=A,B} \chi_i \hat{a}^\dagger \hat{a} \hat{\sigma}_z^i, \tag{2}$$

where $\chi_{A(B)} = \Omega^2 / \delta_{A(B)}$. The above equation can also be obtained by the Fröhlich–Nakajima transformation [82,83]. The standard Dicke Hamiltonian describing the interaction of N identical two-level atoms with a single-mode optical field reads

$$\hat{H}_D = \omega_a \hat{a}^\dagger \hat{a} + \omega \hat{J}_z + \frac{\lambda}{\sqrt{N}} (\hat{a}^\dagger + \hat{a}) (\hat{J}_+ + \hat{J}_-), \tag{3}$$

where ω is the transition frequency of these N identical two-level atoms. \hat{J}_α ($\alpha = x, y, z$) is the collective angular momentum operator for the spin ensemble consisting of N identical two-level atoms; these operators $\hat{J}_x, \hat{J}_y, \hat{J}_z$ satisfy the commutation relation of $SU(2)$ algebra and $\hat{J}_\pm = \hat{J}_x \pm i\hat{J}_y$. When the coupling strength λ exceeds $\sqrt{\omega_a \omega} / 2$, the standard Dicke model exhibits a ground state quantum phase transition from the normal phase to the superradiant phase in the thermodynamic limit $N \rightarrow \infty$ [44–52].

Under the above large detuning condition, the Hamiltonian of the total system as shown in Figure 1 is

$$\hat{H} = \hat{H}_D + \sum_{i=A,B} \frac{\omega_i + \chi_i}{2} \hat{\sigma}_z^i + \sum_{i=A,B} \chi_i \hat{a}^\dagger \hat{a} \hat{\sigma}_z^i. \tag{4}$$

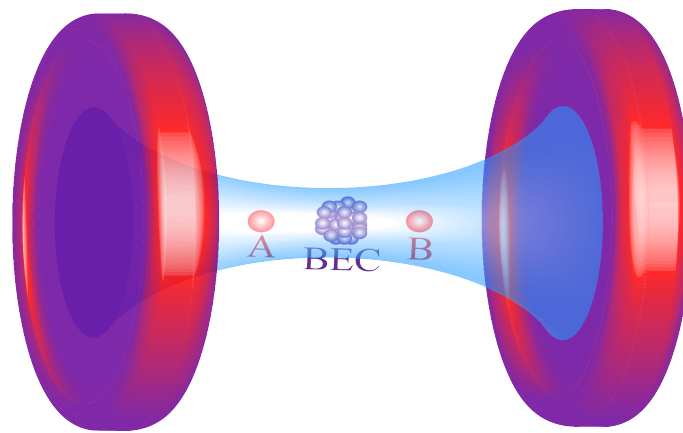


Figure 1. Schematic diagram of the model we used. The N identical two-level atoms marked in purple with a single-mode optical field form the standard Dicke model. A and B denote two impurity qubits, and the two qubits interact only with the optical field. Experimentally, N identical two-level atoms can be realized by Bose–Einstein condensates.

From the above equation, we can see that, since $[\hat{\sigma}_z^A + \hat{\sigma}_z^B, \hat{H}] = [\hat{\sigma}_z^A + \hat{\sigma}_z^B, \hat{H}_D] = 0$, there is no energy exchange between the TIQs and the optical field, and the cavity-BEC system only has an effect on the phase of the two qubits. Therefore, the cavity-BEC system is equivalent to a controlled dephasing environment for the TIQs. In the following, we start to investigate the effect of the Dicke quantum phase transition of the cavity-BEC system on the Berry phase of the TIQs.

We assume that the initial state of the TIQs is a general X-type state with three parameters $\hat{\rho}_{AB}(0) = (\hat{I}^{AB} + \sum_{i=1}^3 c_i \hat{\sigma}_i^A \otimes \hat{\sigma}_i^B)$, where \hat{I}^{AB} is the four-dimensional identity operator; $i = 1, 2, 3$ denotes x, y , and z , respectively. c_i ($0 \leq |c_i| \leq 1$) are real numbers, and they make

the trace of the density matrix $\hat{\rho}_{AB}(0)$ equal to 1 and satisfy the positivity conditions [60]. In the basis $|ee\rangle, |eg\rangle, |ge\rangle, |gg\rangle$, the X-type state is given by

$$\hat{\rho}_{AB}(0) = \frac{1}{4} \begin{pmatrix} 1 + c_3 & 0 & 0 & c_1 - c_2 \\ 0 & 1 - c_3 & c_1 + c_2 & 0 \\ 0 & c_1 + c_2 & 1 - c_3 & 0 \\ c_1 - c_2 & 0 & 0 & 1 + c_3 \end{pmatrix}. \tag{5}$$

The initial state of the cavity-BEC atomic system is the ground state $|G\rangle$ of the standard Dicke Hamiltonian. Then, the density matrix of the total system at time t is

$$\hat{\rho}(t) = \hat{U}(\hat{\rho}_{AB}(0) \otimes |G\rangle\langle G|)\hat{U}^\dagger, \tag{6}$$

where $\hat{U} = \exp(-i\hat{H}t)$.

The density matrix of the TIQs at time t is [60]

$$\begin{aligned} \hat{\rho}_{AB}(t) &= Tr_{cavity-BEC}[\hat{\rho}(t)] \\ &= \frac{1}{4} \begin{pmatrix} 1 + c_3 & 0 & 0 & u(t)D_1(t) \\ 0 & 1 - c_3 & v(t)D_2(t) & 0 \\ 0 & v^*(t)D_2^*(t) & 1 - c_3 & 0 \\ u^*(t)D_1^*(t) & 0 & 0 & 1 + c_3 \end{pmatrix}, \end{aligned} \tag{7}$$

where

$$u(t) = (c_1 - c_2) \exp[-i(\omega'_A + \omega'_B)t], \tag{8}$$

$$v(t) = (c_1 + c_2) \exp[-i(\omega'_A - \omega'_B)t], \tag{9}$$

$$D_1(t) = \exp(2i\delta_1 t \langle G|\hat{a}^\dagger \hat{a}|G\rangle) \exp(-2r\delta_1^2 t^2), \tag{10}$$

$$D_2(t) = \exp(2i\delta_2 t \langle G|\hat{a}^\dagger \hat{a}|G\rangle) \exp(-2r\delta_2^2 t^2), \tag{11}$$

and $\omega'_{A(B)} = \omega_{A(B)} + \chi_{A(B)}$, $\delta_1 = \chi_A + \chi_B$, $\delta_2 = \chi_A - \chi_B$. $\langle G|\hat{a}^\dagger \hat{a}|G\rangle$ and r denote the mean and variance of the light field number operator $\hat{a}^\dagger \hat{a}$ over the ground state of the standard Dicke Hamiltonian, respectively. In the above equation, we use both the $\delta_1 t \ll 1$ and $\delta_2 t \ll 1$ conditions. In the later discussion, we will take these two values as $\delta_1 = 0.0001\omega$ and $\delta_2 = 0$.

After obtaining the density matrix of the TIQs at time t , we study the effect of the Dicke quantum phase transition on the Berry phase of the TIQs in the following. In 2004, Tong et al. gave a definition of the Berry phase of the target system described by the density matrix in open systems [14]. Since this definition is canonically invariant and can be measured by interferometric experiments, it is widely used in the calculation of the Berry phase of mixed state systems. We rewrite the density matrix $\hat{\rho}_{AB}(t)$ in its eigenspace in the following diagonal form

$$\hat{\rho}_{AB}(t) = \sum_{k=1}^{N=4} \epsilon_k(t) |\phi_k(t)\rangle\langle\phi_k(t)|, \tag{12}$$

where N denotes the Hilbert space dimension of the target system and $\epsilon_k(t)$ and $|\phi_k(t)\rangle$ are the eigenvalues and eigenstates of the density matrix $\hat{\rho}_{AB}(t)$, respectively.

Then, the expression for the Berry phase of the mixed state under this non-unitary evolution is defined as follows [14]:

$$\gamma_g(t) = \arg \left[\sum_{k=1}^{N=4} G_k(t) \right] \in (-\pi, \pi], \tag{13}$$

where $G_k(t) = \sqrt{\epsilon_k(0)\epsilon_k(t)} \langle\phi_k(0)|\phi_k(t)\rangle \exp \left[-\int_0^t \langle\phi_k(\tau)|\frac{d}{d\tau}\phi_k(\tau)\rangle d\tau \right]$.

To calculate the Berry phase of the above equation, we need to obtain the eigenvalues and eigenstates of the density matrix $\hat{\rho}_{AB}(t)$. We can obtain all the eigenvalues and the corresponding eigenstates of $\hat{\rho}_{AB}(t)$ from Equation (7) as

$$\epsilon_1(t) = \frac{1}{4} \left(1 - c_3 - |c_1 + c_2| \exp(-2r\delta_2^2 t^2) \right), \tag{14}$$

$$|\phi_1(t)\rangle = \left[0, \frac{-(c_1+c_2) \exp[i[2\delta_2 \langle G|a^\dagger a|G\rangle - (\omega'_A - \omega'_B)]t]}{|c_1+c_2|}, 1, 0 \right]^T, \tag{15}$$

$$\epsilon_2(t) = \frac{1}{4} \left(1 - c_3 + |c_1 + c_2| \exp(-2r\delta_2^2 t^2) \right), \tag{16}$$

$$|\phi_2(t)\rangle = \left[0, \frac{(c_1+c_2) \exp[i[2\delta_2 \langle G|a^\dagger a|G\rangle - (\omega'_A - \omega'_B)]t]}{|c_1+c_2|}, 1, 0 \right]^T, \tag{17}$$

$$\epsilon_3(t) = \frac{1}{4} \left(1 + c_3 - |c_1 - c_2| \exp(-2r\delta_1^2 t^2) \right), \tag{18}$$

$$|\phi_3(t)\rangle = \left[\frac{-(c_1-c_2) \exp[i[2\delta_1 \langle G|a^\dagger a|G\rangle - (\omega'_A + \omega'_B)]t]}{|c_1-c_2|}, 0, 0, 1 \right]^T, \tag{19}$$

$$\epsilon_4(t) = \frac{1}{4} \left(1 + c_3 + |c_1 - c_2| \exp(-2r\delta_1^2 t^2) \right), \tag{20}$$

$$|\phi_4(t)\rangle = \left[\frac{(c_1-c_2) \exp[i[2\delta_1 \langle G|a^\dagger a|G\rangle - (\omega'_A + \omega'_B)]t]}{|c_1-c_2|}, 0, 0, 1 \right]^T. \tag{21}$$

where the “T” in the upper right corner of the matrix indicates a transpose operation on the matrix.

Substituting Equations (14)–(21) into Equation (13), we can obtain the following four expressions:

$$\begin{aligned} G_1(t) &= \sqrt{\epsilon_1(0)\epsilon_1(t)} \langle \phi_1(0) | \phi_1(t) \rangle \exp \left[- \int_0^t \langle \phi_1(\tau) | \frac{d}{d\tau} \phi_1(\tau) \rangle d\tau \right] \\ &= \frac{1}{4} \sqrt{(1 - c_3 - |c_1 + c_2|)(1 - c_3 - |c_1 + c_2| \exp(-2r\delta_2^2 t^2))} \\ &\quad \times \left[1 + \exp \left[-i \left(2\delta_2 \langle G|a^\dagger a|G\rangle - (\omega'_A - \omega'_B) \right) t \right] \right], \end{aligned} \tag{22}$$

$$\begin{aligned} G_2(t) &= \sqrt{\epsilon_2(0)\epsilon_2(t)} \langle \phi_2(0) | \phi_2(t) \rangle \exp \left[- \int_0^t \langle \phi_2(\tau) | \frac{d}{d\tau} \phi_2(\tau) \rangle d\tau \right] \\ &= \frac{1}{4} \sqrt{(1 - c_3 + |c_1 + c_2|)(1 - c_3 + |c_1 + c_2| \exp(-2r\delta_2^2 t^2))} \\ &\quad \times \left[1 + \exp \left[-i \left(2\delta_2 \langle G|a^\dagger a|G\rangle - (\omega'_A - \omega'_B) \right) t \right] \right], \end{aligned} \tag{23}$$

$$\begin{aligned} G_3(t) &= \sqrt{\epsilon_3(0)\epsilon_3(t)} \langle \phi_3(0) | \phi_3(t) \rangle \exp \left[- \int_0^t \langle \phi_3(\tau) | \frac{d}{d\tau} \phi_3(\tau) \rangle d\tau \right] \\ &= \frac{1}{4} \sqrt{(1 + c_3 - |c_1 - c_2|)(1 + c_3 - |c_1 - c_2| \exp(-2r\delta_1^2 t^2))} \\ &\quad \times \left[1 + \exp \left[-i \left(2\delta_1 \langle G|a^\dagger a|G\rangle - (\omega'_A + \omega'_B) \right) t \right] \right], \end{aligned} \tag{24}$$

$$\begin{aligned} G_4(t) &= \sqrt{\epsilon_4(0)\epsilon_4(t)} \langle \phi_4(0) | \phi_4(t) \rangle \exp \left[- \int_0^t \langle \phi_4(\tau) | \frac{d}{d\tau} \phi_4(\tau) \rangle d\tau \right] \\ &= \frac{1}{4} \sqrt{(1 + c_3 + |c_1 - c_2|)(1 + c_3 + |c_1 - c_2| \exp(-2r\delta_1^2 t^2))} \\ &\quad \times \left[1 + \exp \left[-i \left(2\delta_1 \langle G|a^\dagger a|G\rangle - (\omega'_A + \omega'_B) \right) t \right] \right]. \end{aligned} \tag{25}$$

Finally, we obtain the Berry phase of the TIQs at time t :

$$\gamma_g(t) = \arg[p + q + p \cos(mt) + q \cos(nt) - i(p \sin(mt) + q \sin(nt))]$$

$$= \arctan\left(\frac{p \sin(mt) + q \sin(nt)}{p + q + p \cos(mt) + q \cos(nt)}\right) \in (-\pi, \pi], \tag{26}$$

where

$$p = \frac{1}{4} \left[\sqrt{(1 - c_3 - |c_1 + c_2|)(1 - c_3 - |c_1 + c_2| \exp(-2r\delta_2^2 t^2))} + \sqrt{(1 - c_3 + |c_1 + c_2|)(1 - c_3 + |c_1 + c_2| \exp(-2r\delta_2^2 t^2))} \right], \tag{27}$$

$$q = \frac{1}{4} \left[\sqrt{(1 + c_3 - |c_1 - c_2|)(1 + c_3 - |c_1 - c_2| \exp(-2r\delta_1^2 t^2))} + \sqrt{(1 + c_3 + |c_1 - c_2|)(1 + c_3 + |c_1 - c_2| \exp(-2r\delta_1^2 t^2))} \right], \tag{28}$$

$$m = 2\delta_2 \langle G|a^\dagger a|G \rangle - (\omega'_A - \omega'_B), \tag{29}$$

$$n = 2\delta_1 \langle G|a^\dagger a|G \rangle - (\omega'_A + \omega'_B). \tag{30}$$

It is worth emphasizing here that the Berry phases of the TIQs are related to the mean and variance of the optical field number operator over the ground state $|G\rangle$ of the Hamiltonian \hat{H}_D . Meanwhile, we can change the ground state of \hat{H}_D by adjusting the coupling strength λ between the cavity field and the BEC atoms, so we can finally control the Berry phase of the TIQs by adjusting this coupling strength. In the following, we discuss the mean and variance of the optical field number operator $\hat{a}^\dagger \hat{a}$ over the ground state $|G\rangle$ of Hamiltonian \hat{H}_D in each parameter region of λ , respectively.

3. Effect of Dicke Quantum Phase Transition on the Berry Phase of Two Impurity Qubits

In the thermodynamic limit $N \rightarrow \infty$, a quantum phase transition exists in the standard Dicke model. When $\lambda < \lambda_c$ ($\lambda_c = \sqrt{\omega_a \omega} / 2$), the number of excitations on the ground state of \hat{H}_D for both the atoms and the light field is small compared to the total atomic number N , and the system is in the normal phase. When $\lambda > \lambda_c$, both the atoms and the light field have macroscopic excitations on the ground state of \hat{H}_D , and the system is in the superradiant phase. In the standard Dicke model, since the first derivative of the ground state energy of the system is continuous with respect to λ , but its second derivative is discontinuous, this quantum phase transition is a ground state second-order phase transition. In order to obtain the mean and variance of the optical field number operator $\hat{a}^\dagger \hat{a}$ in different parameter regions of λ , in the following, we briefly introduce the ground state in the normal phase region and the superradiant region of the Dicke Hamiltonian, respectively.

Using the Holstein–Primakoff transformation, we can represent the angular momentum operator by the single-mode boson operator as follows [84–86]:

$$\hat{j}_z = \hat{b}^\dagger \hat{b} - \frac{N}{2}, \quad \hat{j}_+ = \hat{b}^\dagger \sqrt{N - \hat{b}^\dagger \hat{b}}, \quad \hat{j}_- = \sqrt{N - \hat{b}^\dagger \hat{b}} \hat{b}, \tag{31}$$

where \hat{b}^\dagger and \hat{b} are the boson creation and annihilation operators, respectively. After substituting Equation (31) into Equation (3) and dropping the constant term, we obtain

$$\hat{H} = \omega_a \hat{a}^\dagger \hat{a} + \omega \hat{b}^\dagger \hat{b} + \lambda (\hat{a}^\dagger + \hat{a}) \left(\hat{b}^\dagger \sqrt{1 - \frac{\hat{b}^\dagger \hat{b}}{N}} + \sqrt{1 - \frac{\hat{b}^\dagger \hat{b}}{N}} \hat{b} \right). \tag{32}$$

In the normal phase, since $\langle G|\hat{b}^\dagger \hat{b}|G\rangle \ll N$, we can obtain the effective Hamiltonian after dropping the constant term:

$$\hat{H}_{np} = \omega_a \hat{a}^\dagger \hat{a} + \omega \hat{b}^\dagger \hat{b} + \lambda (\hat{a}^\dagger + \hat{a}) (\hat{b}^\dagger + \hat{b}). \tag{33}$$

Using the following Bogoliubov transform:

$$\hat{a}^\dagger = f_1 \hat{c}_1^\dagger + f_2 \hat{c}_1 + f_3 \hat{c}_2^\dagger + f_4 \hat{c}_2, \tag{34}$$

$$\hat{b}^\dagger = h_1 \hat{c}_1^\dagger + h_2 \hat{c}_1 + h_3 \hat{c}_2^\dagger + h_4 \hat{c}_2, \tag{35}$$

we can obtain the final diagonal form of \hat{H}_{np} after dropping the constant term:

$$\hat{H}_{np}^d = \epsilon_- \hat{c}_1^\dagger \hat{c}_1 + \epsilon_+ \hat{c}_2^\dagger \hat{c}_2, \tag{36}$$

where

$$\epsilon_\pm^2 = \frac{1}{2} \left[\omega_a^2 + \omega^2 \pm \sqrt{(\omega^2 - \omega_a^2)^2 + 16\lambda^2 \omega_a \omega} \right], \tag{37}$$

$$f_{1,2} = \frac{\cos \theta}{2\sqrt{\epsilon_- \omega_a}} (\omega_a \pm \epsilon_-), \quad f_{3,4} = \frac{\sin \theta}{2\sqrt{\epsilon_+ \omega_a}} (\omega_a \pm \epsilon_+), \tag{38}$$

$$h_{1,2} = -\frac{\sin \theta}{2\sqrt{\epsilon_- \omega}} (\omega \pm \epsilon_-), \quad h_{3,4} = \frac{\cos \theta}{2\sqrt{\epsilon_+ \omega}} (\omega \pm \epsilon_+), \tag{39}$$

and θ is determined by $\tan(2\theta) = \frac{4\lambda\sqrt{\omega_a\omega}}{\omega^2 - \omega_a^2}$.

From Equation (36), we easily obtain that the ground state of the Hamiltonian \hat{H}_{np}^d is $|G\rangle = |0\rangle_{\hat{c}_1} \otimes |0\rangle_{\hat{c}_2} = |0,0\rangle_{\hat{c}_1, \hat{c}_2}$. Here, $|0\rangle_{\hat{c}_1}$ and $|0\rangle_{\hat{c}_2}$ are the ground states of the number operators $\hat{c}_1^\dagger \hat{c}_1$ and $\hat{c}_2^\dagger \hat{c}_2$, respectively.

With Equation (34) and Equation (35), we can easily obtain the mean value and variance of the light field number operator on the ground state of the normal phase:

$$\langle G | \hat{a}^\dagger \hat{a} | G \rangle = f_2^2 + f_4^2, \tag{40}$$

$$\begin{aligned} r &= \langle G | (\hat{a}^\dagger \hat{a})^2 | G \rangle - \left(\langle G | \hat{a}^\dagger \hat{a} | G \rangle \right)^2 \\ &= 2f_1^2 f_2^2 + 2f_3^2 f_4^2 + (f_1 f_4 + f_2 f_3)^2. \end{aligned} \tag{41}$$

When $\lambda > \lambda_c$, the cavity-BEC system is in the superradiant phase. At this point, there is macroscopic excitation of both the atoms and the optical field. We use the displace transformation $\hat{a}^\dagger \rightarrow \hat{a}'^\dagger + \sqrt{\alpha}$ and $\hat{b}^\dagger \rightarrow \hat{b}'^\dagger - \sqrt{\beta}$ such that $\langle G | \hat{b}'^\dagger \hat{b}' | G \rangle \ll N$. Two displacements can be obtained through the equilibrium condition as $\sqrt{\alpha} = \frac{2\lambda}{\omega_a} \sqrt{N(1 - \xi^2)}/4$ and $\sqrt{\beta} = \sqrt{N(1 - \xi)}/2$, where $\xi = \frac{\omega_a \omega}{4\lambda^2}$. Substituting the operators after the displace transformation into Equation (32), dropping the constant term, and in the thermodynamic limit, we can obtain the effective Hamiltonian for the superradiant phase region

$$\hat{H}_{sp} = \omega_a \hat{a}'^\dagger \hat{a}' + \omega' \hat{b}'^\dagger \hat{b}' + \lambda' (\hat{a}'^\dagger + \hat{a}') (\hat{b}'^\dagger + \hat{b}') + \eta (\hat{b}'^\dagger + \hat{b}')^2, \tag{42}$$

where

$$\omega' = \frac{\omega}{2\xi} (1 + \xi), \quad \lambda' = \lambda \xi \sqrt{\frac{2}{1 + \xi}}, \quad \eta = \frac{\omega(1 - \xi)(3 + \xi)}{8\xi(1 + \xi)}. \tag{43}$$

As with the normal phase, using the following Bogoliubov transformation:

$$\hat{a}'^\dagger = f'_1 \hat{c}'_1^\dagger + f'_2 \hat{c}'_1 + f'_3 \hat{c}'_2^\dagger + f'_4 \hat{c}'_2, \tag{44}$$

$$\hat{b}'^\dagger = h'_1 \hat{c}'_1^\dagger + h'_2 \hat{c}'_1 + h'_3 \hat{c}'_2^\dagger + h'_4 \hat{c}'_2. \tag{45}$$

Equation (42) can be written in the following diagonal form after dropping the constant term

$$\hat{H}_{sp}^d = \epsilon'_- \hat{c}'_1^\dagger \hat{c}'_1 + \epsilon'_+ \hat{c}'_2^\dagger \hat{c}'_2, \tag{46}$$

where

$$\epsilon'_{\pm} = \frac{1}{2} \left[\omega_a^2 + \frac{\omega^2}{\xi^2} \pm \sqrt{\left(\frac{\omega^2}{\xi^2} - \omega_a^2\right)^2 + 4\omega_a^2\omega^2} \right], \tag{47}$$

$$f'_{1,2} = \frac{\cos \theta'}{2\sqrt{\epsilon'_-\omega_a}} (\omega_a \pm \epsilon'_-), \quad f'_{3,4} = \frac{\sin \theta'}{2\sqrt{\epsilon'_+\omega_a}} (\omega_a \pm \epsilon'_+), \tag{48}$$

$$h'_{1,2} = -\frac{\sin \theta'}{2\sqrt{\epsilon'_-\omega'}} (\omega' \pm \epsilon'_-), \quad h'_{3,4} = \frac{\cos \theta'}{2\sqrt{\epsilon'_+\omega'}} (\omega' \pm \epsilon'_+), \tag{49}$$

and θ' is determined by $\tan(2\theta') = \frac{2\omega_a\omega\xi^2}{\omega^2 - \xi^2\omega_a^2}$.

Similarly, from Equation (46), we easily obtain that the ground state of Hamiltonian \hat{H}_{sp}^d is $|G\rangle = |0\rangle_{\hat{c}_1} \otimes |0\rangle_{\hat{c}_2} = |0,0\rangle_{\hat{c}_1, \hat{c}_2}$, where $|0\rangle_{\hat{c}_1}$ and $|0\rangle_{\hat{c}_2}$ are the ground states of the number operators $\hat{c}_1^\dagger \hat{c}_1$ and $\hat{c}_2^\dagger \hat{c}_2$, respectively. Thus, we immediately obtain the average and variance of the light field number operators $\hat{a}^\dagger \hat{a}$ in the superradiant phase:

$$\langle G | \hat{a}^\dagger \hat{a} | G \rangle = f_2'^2 + f_4'^2 + \alpha, \tag{50}$$

$$r = \langle G | (\hat{a}^\dagger \hat{a})^2 | G \rangle - \left(\langle G | \hat{a}^\dagger \hat{a} | G \rangle \right)^2 = 2f_1'^2 f_2'^2 + 2f_3'^2 f_4'^2 + (f_1' f_4' + f_2' f_3')^2 + \alpha \left[(f_1' + f_2')^2 + (f_3' + f_4')^2 \right]. \tag{51}$$

In summary, when the coupling intensity λ takes different values, the mean and variance of the number operator $\hat{a}^\dagger \hat{a}$ of the optical field are

$$\langle G | \hat{a}^\dagger \hat{a} | G \rangle = \begin{cases} f_2^2 + f_4^3, & \lambda < \lambda_c, \\ f_2'^2 + f_4'^2 + \alpha, & \lambda > \lambda_c, \end{cases} \tag{52}$$

$$r = \begin{cases} 2f_1^2 f_2^2 + 2f_3^4 f_4^3 + (f_1 f_4 + f_2 f_3)^2, & \lambda < \lambda_c, \\ 2f_1'^2 f_2'^2 + 2f_3'^2 f_4'^2 + (f_1' f_4' + f_2' f_3')^2 + \alpha \left[(f_1' + f_2')^2 + (f_3' + f_4')^2 \right], & \lambda > \lambda_c. \end{cases} \tag{53}$$

The variation of the Berry phase of the TIQs with the phase transition parameter λ is obtained by substituting Equations (52) and (53) into Equation (26). In the following, we discuss the effect of the Dicke quantum phase transition on the Berry phase of the TIQs.

In Figure 2a,c,e, we plot the variation of the Berry phase with the phase transition parameter λ for the TIQs, respectively. We find that at these three different times, the Berry phase of the TIQs shows a sudden change at the critical point of the phase transition parameter λ when the TIQs take different initial values. In Figure 2b,d,f, we plot the variation of the Berry phase of the TIQs with the phase transition parameter λ and the initial condition c_1 , respectively. At the three different times, we find that the Berry phase of the TIQs undergoes a sudden change at the critical phase transition point λ_c , and the Berry phase of the TIQs changes differently near the critical phase transition point λ_c at different times. For example, when $t = 1/\omega$, the Berry phase of the TIQs gradually decreases when the phase transition parameter λ leaves the phase transition critical value λ_c . When $t = 1.3/\omega$, the Berry phase of the TIQs first gradually decreases and then gradually increases when the phase transition parameter λ leaves the phase transition point. When $t = 2/\omega$, the Berry phase of the TIQs keeps increasing when the phase transition parameter λ leaves the critical value λ_c . To explain the different behaviors of the Berry phases of the TIQs above near the critical coupling strength λ_c , we plot the changes of the Berry phases of the TIQs with the phase transition parameter λ and time t in Figure 3. We find that, at any time, the Berry phase of the two qubits undergoes a sudden change in the phase transition point. Therefore, we can take the abrupt change of the Berry phase of the TIQs as a phase transition signal of the Dicke quantum phase transition. In addition, at the phase transition point, we find that the Berry phase of the TIQs decreases with increasing time t .

However, when $\lambda \neq \lambda_c$, the Berry phase of the TIQs decreases first and then increases with time t . These two phenomena then lead to different changes in the Berry phase of the TIQs near the phase transition point at different times in Figure 2b,d,f.

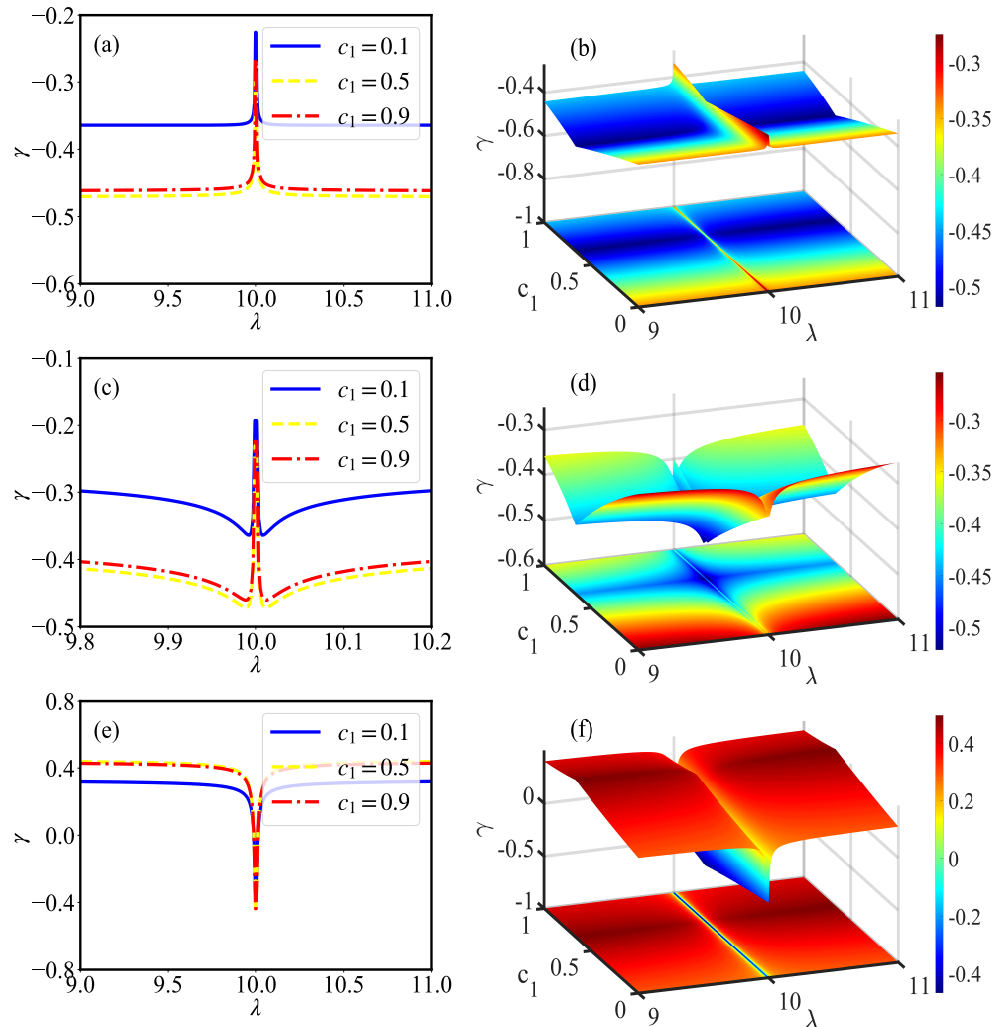


Figure 2. (a,c,e) Variation of the Berry phase γ of the TIQs with the phase transition parameter λ when $t = 1/\omega$, $t = 1.3/\omega$, $t = 2/\omega$, respectively. (b,d,f) Variation of the Berry phase γ of the TIQs with their initial state parameter c_1 and phase transition parameter λ when $t = 1/\omega$, $t = 1.3/\omega$, $t = 2/\omega$, respectively. The other parameters are $c_2 = 0$, $c_3 = 0.5c_1$, $\omega_a = 400\omega$, $\delta_1 = 0.0001\omega$, $\delta_2 = 0$, $\omega_A = \omega_B = \omega$, $\lambda_c = \sqrt{\omega\omega_a}/2 = 10\omega$, and $N = 10^5$.

Meanwhile, we found another interesting phenomenon in Figure 2b,d,f. In Figure 2b,d, by observing the variation of the Berry phase with the initial condition c_1 , we find that the Berry phase always takes the minimum value when c_1 is equal to a certain value. Furthermore, in Figure 2f, we find that the Berry phase always takes the maximum value when c_1 equals this value. To investigate this interesting phenomenon, in Figure 4, we plot the variation of the Berry phase of the two qubits with the initial state parameter c_1 for different values of the phase transition parameter when the time takes different values. We find that the Berry phase of the two qubits always changes abruptly at the point $c_1 = 2/3$ for different phase transition parameters and times. Therefore, in the cavity-BEC system with TIQs, both the phase transition parameter λ and the initial state value c_1 of the two qubits cause abrupt changes in the Berry phase of the TIQs.

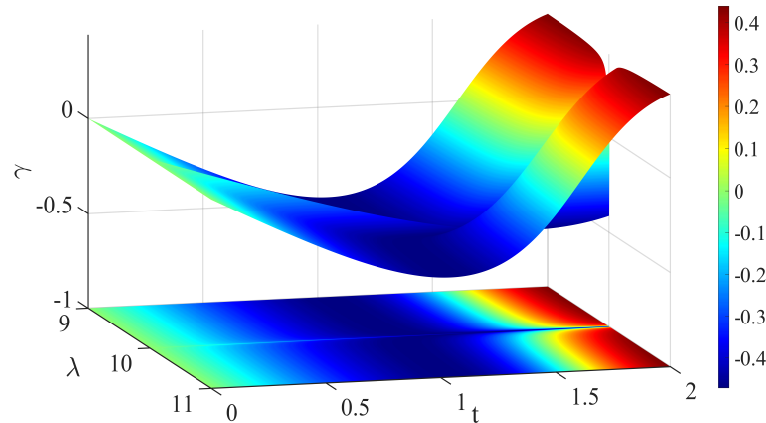


Figure 3. Berry phase of the TIQs varies with the phase transition parameter λ and time t when $c_1 = 0.5$. The other parameters are the same as in Figure 2, and all parameters are in units of ω .

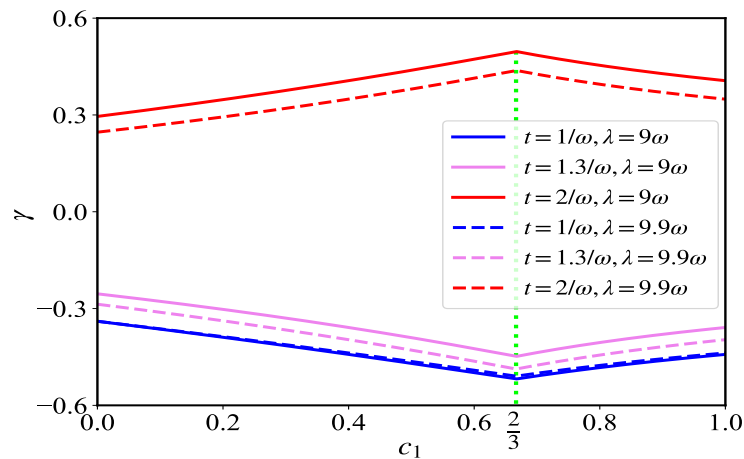


Figure 4. Berry phase of the TIQs varies with the initial state parameter c_1 for different phase transition parameters λ and times t . The other parameters are the same as in Figure 2.

Experimentally, the Dicke quantum phase transition has been realized in a system consisting of a BEC coupled to an optical cavity [49]. Meanwhile, manipulating atoms by optical fields based on a cavity-quantum-electrodynamics system is already a well-established technique [87–91]. Moreover, the Berry phase of the qubit can be measured experimentally [10,92,93]. Therefore, the characterization of Dicke quantum phase transitions by the Berry phase of the TIQs is experimentally feasible.

4. Conclusions

We mainly studied the effect of the Dicke quantum phase transition on the Berry phase of the two impurity qubits. When the two impurity qubits only have a dispersive interaction with the optical field of the Dicke model, the two impurity qubits do not affect the ground state quantum phase transition of the Dicke model. We find that the Berry phase of the two impurity qubits is closely related to the mean and variance of the optical field number operator in the Dicke model over the ground state. By studying the mean and variance of the optical field number operator in the normal and superradiant phases, we find that the two impurity qubits Berry phase has a sudden change at the phase transition point at any time. Therefore, the Berry phase of the two impurity qubits can be used as a phase transition signal for the Dicke quantum phase transition. In addition, we found that the two impurity qubits behave differently near the phase transition point at different times. We explained the reason for the appearance of this different behavior by studying

the variation of the Berry phase with the phase transition parameters and time. Finally, we found that the Berry phase of the two impurity qubits also has a sudden change at some initial value. In this article, we focused on the effect of the Dicke quantum phase transition on the Berry phase of the two qubits. The initial entanglement of the two qubits, the entanglement of the optical field and the BEC, and the frequency detuning between the optical field and the condensed atoms also affect the Berry phase of the two qubits, and we will study these in our next work.

Author Contributions: Conceptualization, W.L. and S.T.; methodology, J.Y. and Y.L.; software, C.Z. and Y.S.; validation, W.L., C.Z., Y.S., Y.S., J.Y. and S.T.; formal analysis, W.L.; investigation, W.L.; resources, W.L., Y.L., Y.S., J.Y. and S.T.; data curation, C.Z.; writing—original draft preparation, W.L. and S.T.; writing—review and editing, W.L. and C.Z.; visualization, C.L. and Y.S.; supervision, W.L.; project administration, W.L.; funding acquisition, W.L. All authors have read and agreed to the published version of the manuscript.

Funding: This work was supported by the NSFC (Grant No. 11947069, No. 11905053, No. 12205092, and No. 12205088), the Scientific Research Fund of Hunan Provincial Education Department (Grant No. 20C0495, No. 21B0639, and No. 21B0647), and the Hunan Provincial Natural Science Foundation of China (Grant No. 2020JJ4146).

Institutional Review Board Statement: Not applicable.

Informed Consent Statement: Not applicable.

Data Availability Statement: Not applicable.

Conflicts of Interest: The authors declare no conflict of interest.

References

1. Berry, M.V. Quantal phase factors accompanying adiabatic changes. *Proc. R. Soc. Lond. A Math. Phys. Sci.* **1984**, *392*, 45–57. [[CrossRef](#)]
2. Simon, B. Holonomy, the Quantum Adiabatic Theorem, and Berry's Phase. *Phys. Rev. Lett.* **1983**, *51*, 2167–2170. [[CrossRef](#)]
3. Anandan, J.; Aharonov, Y. Geometry of quantum evolution. *Phys. Rev. Lett.* **1990**, *65*, 1697–1700. [[CrossRef](#)] [[PubMed](#)]
4. Pancharatnam, S. Generalized theory of interference and its applications. *Proc. Indian Acad. Sci.* **1956**, *44*, 398–417. [[CrossRef](#)]
5. Cohen, E.; Larocque, H.; Bouchard, F.; Nejdassattari, F.; Gefen, Y.; Karimi, E. Geometric phase from Aharonov–Bohm to Pancharatnam–Berry and beyond. *Nat. Rev. Phys.* **2019**, *1*, 437–449. [[CrossRef](#)]
6. Samuel, J.; Bhandari, R. General Setting for Berry's Phase. *Phys. Rev. Lett.* **1988**, *60*, 2339–2342. [[CrossRef](#)]
7. Tomita, A.; Chiao, R.Y. Observation of Berry's Topological Phase by Use of an Optical Fiber. *Phys. Rev. Lett.* **1986**, *57*, 937–940. [[CrossRef](#)]
8. Du, J.; Zhu, J.; Shi, M.; Peng, X.; Suter, D. Experimental observation of a topological phase in the maximally entangled state of a pair of qubits. *Phys. Rev. A* **2007**, *76*, 042121. [[CrossRef](#)]
9. Chen, H.; Hu, M.; Chen, J.; Du, J. Observation of geometric phases for three-level systems using NMR interferometry. *Phys. Rev. A* **2009**, *80*, 054101. [[CrossRef](#)]
10. Leek, P.J.; Fink, J.; Blais, A.; Bianchetti, R.; Goppl, M.; Gambetta, J.M.; Schuster, D.I.; Frunzio, L.; Schoelkopf, R.J.; Wallraff, A. Observation of Berry's phase in a solid-state qubit. *Science* **2007**, *318*, 1889–1892. [[CrossRef](#)]
11. Möttönen, M.; Vartiainen, J.J.; Pekola, J.P. Experimental Determination of the Berry Phase in a Superconducting Charge Pump. *Phys. Rev. Lett.* **2008**, *100*, 177201. [[CrossRef](#)]
12. Sjöqvist, E.; Pati, A.K.; Ekert, A.; Anandan, J.S.; Ericsson, M.; Oi, D.K.L.; Vedral, V. Geometric Phases for Mixed States in Interferometry. *Phys. Rev. Lett.* **2000**, *85*, 2845–2849. [[CrossRef](#)]
13. Ericsson, M.; Achilles, D.; Barreiro, J.T.; Branning, D.; Peters, N.A.; Kwiat, P.G. Measurement of Geometric Phase for Mixed States Using Single Photon Interferometry. *Phys. Rev. Lett.* **2005**, *94*, 050401. [[CrossRef](#)]
14. Tong, D.M.; Sjöqvist, E.; Kwek, L.C.; Oh, C.H. Kinematic Approach to the Mixed State Geometric Phase in Nonunitary Evolution. *Phys. Rev. Lett.* **2004**, *93*, 080405. [[CrossRef](#)]
15. Ekert, A.; Ericsson, M.; Hayden, P.; Inamori, H.; Jones, J.A.; Oi, D.K.; Vedral, V. Geometric quantum computation. *J. Mod. Opt.* **2000**, *47*, 2501–2513. [[CrossRef](#)]
16. Zanardi, P.; Rasetti, M. Holonomic quantum computation. *Phys. Lett. A* **1999**, *264*, 94–99. [[CrossRef](#)]
17. Zhu, S.L.; Wang, Z.D. Implementation of Universal Quantum Gates Based on Nonadiabatic Geometric Phases. *Phys. Rev. Lett.* **2002**, *89*, 097902. [[CrossRef](#)]
18. Zhu, S.L.; Wang, Z.D. Unconventional Geometric Quantum Computation. *Phys. Rev. Lett.* **2003**, *91*, 187902. [[CrossRef](#)]
19. Huang, H.Y.; Broughton, M.; Cotler, J.; Chen, S.; Li, J.; Mohseni, M.; Neven, H.; Babbush, R.; Kueng, R.; Preskill, J.; et al. Quantum advantage in learning from experiments. *Science* **2022**, *376*, 1182–1186. [[CrossRef](#)]

20. Zhou, M.G.; Cao, X.Y.; Lu, Y.S.; Wang, Y.; Bao, Y.; Jia, Z.Y.; Fu, Y.; Yin, H.L.; Chen, Z.B. Experimental quantum advantage with quantum coupon collector. *Research* **2022**, *2022*, 9798679. [[CrossRef](#)]
21. Xie, Y.M.; Lu, Y.S.; Weng, C.X.; Cao, X.Y.; Jia, Z.Y.; Bao, Y.; Wang, Y.; Fu, Y.; Yin, H.L.; Chen, Z.B. Breaking the Rate-Loss Bound of Quantum Key Distribution with Asynchronous Two-Photon Interference. *PRX Quantum* **2022**, *3*, 020315. [[CrossRef](#)]
22. Zhou, N.R.; Zhang, T.F.; Xie, X.W.; Wu, J.Y. Hybrid quantum–classical generative adversarial networks for image generation via learning discrete distribution. *Signal Process. Image Commun.* **2022**, 116891. *in press*. [[CrossRef](#)]
23. Azimi Mousolou, V.; Canali, C.M.; Sjöqvist, E. Unifying geometric entanglement and geometric phase in a quantum phase transition. *Phys. Rev. A* **2013**, *88*, 012310. [[CrossRef](#)]
24. Cui, H.T.; Yi, J. Geometric phase and quantum phase transition: Two-band model. *Phys. Rev. A* **2008**, *78*, 022101. [[CrossRef](#)]
25. Ma, Y.Q.; Chen, S. Geometric phase and quantum phase transition in an inhomogeneous periodic XY spin- $\frac{1}{2}$ model. *Phys. Rev. A* **2009**, *79*, 022116. [[CrossRef](#)]
26. Nesterov, A.I.; Ovchinnikov, S.G. Geometric phases and quantum phase transitions in open systems. *Phys. Rev. E* **2008**, *78*, 015202. [[CrossRef](#)]
27. Carollo, A.C.M.; Pachos, J.K. Geometric Phases and Criticality in Spin-Chain Systems. *Phys. Rev. Lett.* **2005**, *95*, 157203. [[CrossRef](#)]
28. Hamma, A. Berry phases and quantum phase transitions. *arXiv* **2006**. arXiv:quant-ph/0602091.
29. Zhu, S.L. Geometric phases and quantum phase transitions. *Int. J. Mod. Phys. B* **2008**, *22*, 561–581. [[CrossRef](#)]
30. Lu, X.M.; Wang, X. Operator quantum geometric tensor and quantum phase transitions. *EPL (Europhys. Lett.)* **2010**, *91*, 30003. [[CrossRef](#)]
31. Pachos, J.K.; Carollo, A.C. Geometric phases and criticality in spin systems. *Philos. Trans. R. Soc. Math. Phys. Eng. Sci.* **2006**, *364*, 3463–3476. [[CrossRef](#)]
32. Plastina, F.; Liberti, G.; Carollo, A. Scaling of Berry’s phase close to the Dicke quantum phase transition. *EPL (Europhys. Lett.)* **2006**, *76*, 182. [[CrossRef](#)]
33. Zhu, S.L. Scaling of Geometric Phases Close to the Quantum Phase Transition in the XY Spin Chain. *Phys. Rev. Lett.* **2006**, *96*, 077206. [[CrossRef](#)]
34. Reuter, M.E.; Hartmann, M.J.; Plenio, M.B. Geometric phases and critical phenomena in a chain of interacting spins. *Proc. R. Soc. A Math. Phys. Eng. Sci.* **2007**, *463*, 1271–1285. [[CrossRef](#)]
35. Peng, X.; Wu, S.; Li, J.; Suter, D.; Du, J. Observation of the Ground-State Geometric Phase in a Heisenberg XY Model. *Phys. Rev. Lett.* **2010**, *105*, 240405. [[CrossRef](#)] [[PubMed](#)]
36. Chen, G.; Li, J.; Liang, J.Q. Critical property of the geometric phase in the Dicke model. *Phys. Rev. A* **2006**, *74*, 054101. [[CrossRef](#)]
37. Cui, H.; Li, K.; Yi, X. Geometric phase and quantum phase transition in the Lipkin–Meshkov–Glick model. *Phys. Lett. A* **2006**, *360*, 243–248. [[CrossRef](#)]
38. Sjöqvist, E.; Rahaman, R.; Basu, U.; Basu, B. Berry phase and fidelity susceptibility of the three-qubit Lipkin–Meshkov–Glick ground state. *J. Phys. Math. Theor.* **2010**, *43*, 354026. [[CrossRef](#)]
39. Guerra, C.A.E.; Mahecha-Gómez, J.; Hirsch, J.G. Quantum phase transition and Berry phase in an extended Dicke model. *Eur. Phys. J. D* **2020**, *74*, 1–7. [[CrossRef](#)]
40. Yuan, Z.G.; Zhang, P.; Li, S.S.; Jing, J.; Kong, L.B. Scaling of the Berry phase close to the excited-state quantum phase transition in the Lipkin model. *Phys. Rev. A* **2012**, *85*, 044102. [[CrossRef](#)]
41. Paunković, N.; Rocha Vieira, V. Macroscopic distinguishability between quantum states defining different phases of matter: Fidelity and the Uhlmann geometric phase. *Phys. Rev. E* **2008**, *77*, 011129. [[CrossRef](#)] [[PubMed](#)]
42. Zhang, L.D.; Fu, L.B. Mean-field Berry phase of an interacting spin-1/2 system. *EPL (Europhys. Lett.)* **2011**, *93*, 30001. [[CrossRef](#)]
43. Carollo, A.; Valenti, D.; Spagnolo, B. Geometry of quantum phase transitions. *Phys. Rep.* **2020**, *838*, 1–72. [[CrossRef](#)]
44. Dicke, R.H. Coherence in Spontaneous Radiation Processes. *Phys. Rev.* **1954**, *93*, 99–110. [[CrossRef](#)]
45. Hepp, K.; Lieb, E.H. On the superradiant phase transition for molecules in a quantized radiation field: the Dicke maser model. *Ann. Phys.* **1973**, *76*, 360–404. [[CrossRef](#)]
46. Hepp, K.; Lieb, E.H. Equilibrium Statistical Mechanics of Matter Interacting with the Quantized Radiation Field. *Phys. Rev. A* **1973**, *8*, 2517–2525. [[CrossRef](#)]
47. Emary, C.; Brandes, T. Quantum Chaos Triggered by Precursors of a Quantum Phase Transition: The Dicke Model. *Phys. Rev. Lett.* **2003**, *90*, 044101. [[CrossRef](#)]
48. Emary, C.; Brandes, T. Chaos and the quantum phase transition in the Dicke model. *Phys. Rev. E* **2003**, *67*, 066203. [[CrossRef](#)]
49. Baumann, K.; Guerlin, C.; Brennecke, F.; Esslinger, T. Dicke quantum phase transition with a superfluid gas in an optical cavity. *Nature* **2010**, *464*, 1301–1306. [[CrossRef](#)]
50. Baumann, K.; Mottl, R.; Brennecke, F.; Esslinger, T. Exploring Symmetry Breaking at the Dicke Quantum Phase Transition. *Phys. Rev. Lett.* **2011**, *107*, 140402. [[CrossRef](#)]
51. Yuan, J.B.; Lu, W.J.; Song, Y.J.; Kuang, L.M. Single-impurity-induced Dicke quantum phase transition in a cavity-Bose–Einstein condensate. *Sci. Rep.* **2017**, *7*, 1–9. [[CrossRef](#)] [[PubMed](#)]
52. Lu, W.J.; Li, Z.; Kuang, L.M. Nonlinear Dicke quantum phase transition and its quantum witness in a cavity-Bose–Einstein-condensate system. *Chin. Phys. Lett.* **2018**, *35*, 116401. [[CrossRef](#)]
53. Li, Z.; Kuang, L.M. Controlling quantum coherence of a two-component Bose–Einstein condensate via an impurity atom. *Quantum Inf. Process.* **2020**, *19*, 1–17. [[CrossRef](#)]

54. Song, Y.J.; Tan, Q.S.; Kuang, L.M. Control quantum evolution speed of a single dephasing qubit for arbitrary initial states via periodic dynamical decoupling pulses. *Sci. Rep.* **2017**, *7*, 43654. [[CrossRef](#)] [[PubMed](#)]
55. Song, Y.J.; Kuang, L.M. Controlling Decoherence Speed Limit of a Single Impurity Atom in a Bose–Einstein-Condensate Reservoir. *Ann. Der Phys.* **2019**, *531*, 1800423. [[CrossRef](#)]
56. Wu, X.; Jiao, Y.F.; Jia, S.P.; Zhang, J.; Zhai, C.L.; Kuang, L.M. Micro–micro and micro–macro entanglement witnessing via the geometric phase in an impurity-doped Bose–Einstein condensate. *Quantum Inf. Process.* **2022**, *21*, 1–20. [[CrossRef](#)]
57. Han, Y.; Li, Z.; Kuang, L.M. Quantum dynamics of an impurity-doped Bose–Einstein condensate system. *Commun. Theor. Phys.* **2020**, *72*, 095102. [[CrossRef](#)]
58. Jia, S.P.; Li, B.; Jiao, Y.F.; Jing, H.; Kuang, L.M. Einstein-Podolsky-Rosen steering of quantum phases in a cavity Bose–Einstein condensate with a single impurity. *arXiv* **2022**, arXiv:2205.13938.
59. Li, Z.; Han, Y.; Kuang, L.M. Complementarity between micro-micro and micro-macro entanglement in a Bose–Einstein condensate with two Rydberg impurities. *Commun. Theor. Phys.* **2020**, *72*, 025101. [[CrossRef](#)]
60. Yuan, J.B.; Kuang, L.M. Quantum-discord amplification induced by a quantum phase transition via a cavity–Bose–Einstein-condensate system. *Phys. Rev. A* **2013**, *87*, 024101. [[CrossRef](#)]
61. Levinsen, J.; Parish, M.M.; Bruun, G.M. Impurity in a Bose–Einstein Condensate and the Efimov Effect. *Phys. Rev. Lett.* **2015**, *115*, 125302. [[CrossRef](#)]
62. Christensen, R.S.; Levinsen, J.; Bruun, G.M. Quasiparticle Properties of a Mobile Impurity in a Bose–Einstein Condensate. *Phys. Rev. Lett.* **2015**, *115*, 160401. [[CrossRef](#)]
63. Lausch, T.; Widera, A.; Fleischhauer, M. Prethermalization in the cooling dynamics of an impurity in a Bose–Einstein condensate. *Phys. Rev. A* **2018**, *97*, 023621. [[CrossRef](#)]
64. Lena, R.G.; Daley, A.J. Dissipative dynamics and cooling rates of trapped impurity atoms immersed in a reservoir gas. *Phys. Rev. A* **2020**, *101*, 033612. [[CrossRef](#)]
65. Yoshida, S.M.; Endo, S.; Levinsen, J.; Parish, M.M. Universality of an Impurity in a Bose–Einstein Condensate. *Phys. Rev. X* **2018**, *8*, 011024. [[CrossRef](#)]
66. Volya, A.; Zelevinsky, V. Invariant correlational entropy as a signature of quantum phase transitions in nuclei. *Phys. Lett. B* **2003**, *574*, 27–34. [[CrossRef](#)]
67. Wang, T.L.; Wu, L.N.; Yang, W.; Jin, G.R.; Lambert, N.; Nori, F. Quantum Fisher information as a signature of the superradiant quantum phase transition. *New J. Phys.* **2014**, *16*, 063039. [[CrossRef](#)]
68. Yang, L.P.; Jacob, Z. Quantum critical detector: amplifying weak signals using discontinuous quantum phase transitions. *Opt. Express* **2019**, *27*, 10482–10494. [[CrossRef](#)]
69. Paunković, N.; Sacramento, P.D.; Nogueira, P.; Vieira, V.R.; Dugaev, V.K. Fidelity between partial states as a signature of quantum phase transitions. *Phys. Rev. A* **2008**, *77*, 052302. [[CrossRef](#)]
70. Relaño, A.; Arias, J.M.; Dukelsky, J.; García-Ramos, J.E.; Pérez-Fernández, P. Decoherence as a signature of an excited-state quantum phase transition. *Phys. Rev. A* **2008**, *78*, 060102. [[CrossRef](#)]
71. Chen, J.J.; Cui, J.; Zhang, Y.R.; Fan, H. Coherence susceptibility as a probe of quantum phase transitions. *Phys. Rev. A* **2016**, *94*, 022112. [[CrossRef](#)]
72. Hu, M.L.; Gao, Y.Y.; Fan, H. Steered quantum coherence as a signature of quantum phase transitions in spin chains. *Phys. Rev. A* **2020**, *101*, 032305. [[CrossRef](#)]
73. Zhou, B.; Yang, C.; Chen, S. Signature of a nonequilibrium quantum phase transition in the long-time average of the Loschmidt echo. *Phys. Rev. B* **2019**, *100*, 184313. [[CrossRef](#)]
74. Wang, Q.; Pérez-Bernal, F. Signatures of excited-state quantum phase transitions in quantum many-body systems: Phase space analysis. *Phys. Rev. E* **2021**, *104*, 034119. [[CrossRef](#)] [[PubMed](#)]
75. Quan, H.T.; Song, Z.; Liu, X.F.; Zanardi, P.; Sun, C.P. Decay of Loschmidt Echo Enhanced by Quantum Criticality. *Phys. Rev. Lett.* **2006**, *96*, 140604. [[CrossRef](#)]
76. Wu, W.; Xu, J.B. Geometric phase, quantum Fisher information, geometric quantum correlation and quantum phase transition in the cavity-Bose–Einstein-condensate system. *Quantum Inf. Process.* **2016**, *15*, 3695–3709. [[CrossRef](#)]
77. Peixoto de Faria, J.G.; Nemes, M.C. Dissipative dynamics of the Jaynes-Cummings model in the dispersive approximation: Analytical results. *Phys. Rev. A* **1999**, *59*, 3918–3925. [[CrossRef](#)]
78. Obada, A.S.; Hessien, H.; Mohamed, A.B. The effects of thermal photons on entanglement dynamics for a dispersive Jaynes–Cummings model. *Phys. Lett. A* **2008**, *372*, 3699–3706. [[CrossRef](#)]
79. Zhang, J.S.; Chen, A.X.; Abdel-Aty, M. Two atoms in dissipative cavities in dispersive limit: entanglement sudden death and long-lived entanglement. *J. Phys. B At. Mol. Opt. Phys.* **2009**, *43*, 025501. [[CrossRef](#)]
80. Ban, M. Exact time-evolution of the dispersive Jaynes–Cummings model: the effect of initial correlation and master equation approach. *J. Mod. Opt.* **2011**, *58*, 640–651. [[CrossRef](#)]
81. Guo, Y.T.; Zou, F.; Huang, J.F.; Liao, J.Q. Retrieval of photon blockade effect in the dispersive Jaynes-Cummings model. *Phys. Rev. A* **2022**, *105*, 013705. [[CrossRef](#)]
82. Fröhlich, H. Theory of the Superconducting State. I. The Ground State at the Absolute Zero of Temperature. *Phys. Rev.* **1950**, *79*, 845–856. [[CrossRef](#)]
83. Nakajima, S. Perturbation theory in statistical mechanics. *Adv. Phys.* **1955**, *4*, 363–380. [[CrossRef](#)]

84. Holstein, T.; Primakoff, H. Field Dependence of the Intrinsic Domain Magnetization of a Ferromagnet. *Phys. Rev.* **1940**, *58*, 1098–1113. [[CrossRef](#)]
85. Ressayre, E.; Tallet, A. Holstein-Primakoff transformation for the study of cooperative emission of radiation. *Phys. Rev. A* **1975**, *11*, 981–988. [[CrossRef](#)]
86. Persico, F.; Vetri, G. Coherence properties of the N -atom-radiation interaction and the Holstein-Primakoff transformation. *Phys. Rev. A* **1975**, *12*, 2083–2091. [[CrossRef](#)]
87. Thompson, R.J.; Rempe, G.; Kimble, H.J. Observation of normal-mode splitting for an atom in an optical cavity. *Phys. Rev. Lett.* **1992**, *68*, 1132–1135. [[CrossRef](#)]
88. Brune, M.; Schmidt-Kaler, F.; Maali, A.; Dreyer, J.; Hagley, E.; Raimond, J.M.; Haroche, S. Quantum Rabi Oscillation: A Direct Test of Field Quantization in a Cavity. *Phys. Rev. Lett.* **1996**, *76*, 1800–1803. [[CrossRef](#)]
89. Kimble, H.J. Strong interactions of single atoms and photons in cavity QED. *Phys. Scr.* **1998**, *1998*, 127. [[CrossRef](#)]
90. Reiserer, A.; Rempe, G. Cavity-based quantum networks with single atoms and optical photons. *Rev. Mod. Phys.* **2015**, *87*, 1379–1418. [[CrossRef](#)]
91. Johnson, A.; Blaha, M.; Ulanov, A.E.; Rauschenbeutel, A.; Schneeweiss, P.; Volz, J. Observation of Collective Superstrong Coupling of Cold Atoms to a 30-m Long Optical Resonator. *Phys. Rev. Lett.* **2019**, *123*, 243602. [[CrossRef](#)] [[PubMed](#)]
92. Lombardo, F.C.; Villar, P.I. Corrections to the Berry phase in a solid-state qubit due to low-frequency noise. *Phys. Rev. A* **2014**, *89*, 012110. [[CrossRef](#)]
93. Zhang, Z.; Wang, T.; Xiang, L.; Yao, J.; Wu, J.; Yin, Y. Measuring the Berry phase in a superconducting phase qubit by a shortcut to adiabaticity. *Phys. Rev. A* **2017**, *95*, 042345. [[CrossRef](#)]